Basolateral Membrane H/OH/HCO_3 Transport in the Rat Cortical Thick Ascending Limb

Evidence for an Electrogenic Na/HCO_3 Cotransporter in Parallel with a Na/H Antiporter

Reto Krapf
Department of Medicine, Cardiovascular Research Institute, University of California, San Francisco, California 94143-0532

Abstract

Mechanisms involved in basolateral H/OH/HCO_3 transport in the in vitro microperfused rat cortical thick ascending limb were examined by the microfluorometric determination of cell pH using (2',7')-*bis*-(carboxyethyl)-(5,6)-carboxyfluorescein. The mean cell pH in this segment perfused with 147 mM sodium and 25 mM HCO_3 at pH 7.4 was 7.13±0.02 (n = 30). Lowering bath HCO_3 from 25 to 5 mM (constant P_{CO_2} of 40 mmHg) acidified the cells by 0.31±0.02 pH units at a rate of 0.56±0.08 pH units/min. Removal of bath sodium acidified the cells by 0.28±0.03 pH units at a rate of 0.33±0.04 pH units/min. The cell acidification was stilbene inhibitable and independent of chloride. There was no effect of bath sodium removal on cell pH in the absence of CO_2/HCO_3. Depolarization of the basolateral membrane (step increase in bath potassium) independent of the presence of chloride. Cell acidification induced by bath sodium removal persisted when the basolateral membrane was voltage clamped by high potassium/valinomycin. Although these results are consistent with a Na/$(HCO_3)_{n>1}$ cotransporter, a Na/H antiporter was also suggested: 1 mM bath amiloride inhibited the cell pH defense against an acid load (rapid ammonia washout), both in the presence and absence of CO_2/HCO_3, and inhibited the cell acidification induced by bath sodium reduction from 50 to 0 mM.

In conclusion, an electrogenic Na/$(HCO_3)_{n>1}$ cotransporter in parallel with a Na/H antiporter exist on the basolateral membrane of the rat cortical thick ascending limb.

Introduction

Free-flow micropuncture studies have established that 50–70% of the bicarbonate (HCO_3) delivered out of the proximal convoluted tubule is reabsorbed in the loop of Henle (1, 2), at a rate of about 35 pmol/min. Although the proximal straight tubule can reabsorb HCO_3, studies by Good (3) and Good et al. (4) have shown that the rat medullary and cortical thick ascending limbs (TAL)[1] reabsorb HCO_3 at a rate of ~ 5–10 pmol/mm · min. These studies have suggested that the TAL, which has a length in the rat of ~ 4 mm, may be the important site of loop of Henle acidification and may have a quantitatively important role in overall renal acidification. Net HCO_3 reabsorption in the TAL correlates with the histochemical evidence for carbonic anhydrase in this segment: rabbit TAL do not reabsorb HCO_3 and are negative for carbonic anhydrase (5, 6), whereas the HCO_3-reabsorbing rat TAL is positive for carbonic anhydrase (7). Interestingly, the human TAL is also positive for carbonic anhydrase (8).

In the rat cortical TAL, HCO_3 reabsorption is sodium dependent, electroneutral, dependent on carbonic anhydrase, and inhibited by luminal amiloride (3), suggesting that a luminal Na/H antiporter effects acidification (3, 9, 10). In addition, evidence has been provided for a luminal Cl/HCO_3 exchanger in the mouse cortical TAL (9).

Net HCO_3 reabsorption in the rat TAL requires basolateral base exit. In comparison to the luminal side less is known about the transport mechanisms involved in H/OH/HCO_3 transport across the basolateral membrane. Studies in the mouse medullary TAL suggest that Na/H and Cl/HCO_3 antiporters are present on the basolateral membrane (11). Although they may be important in vasopressin-dependent hypertonic cell volume regulation, their role in cell pH regulation and transepithelial base reabsorption is unknown. Evidence has also been provided recently for an electrogenic sodium-dependent HCO_3 cotransport mechanism in fused cells from the frog kidney diluting segment (12, 13), a segment that shares many similarities with the mammalian TAL.

Therefore, the purpose of this study was to examine mechanisms of basolateral H/OH/HCO_3 transport in the rat cortical TAL. The technique of measuring cell pH with the pH-sensitive dye, (2',7')-*bis*-(carboxyethyl)-(5,6)-carboxyfluorescein (BCECF), was adapted to the in vitro microperfused rat cortical TAL.

The results provide evidence for the existence of an electrogenic, stilbene-sensitive Na/$(HCO_3)_{n>1}$ cotransporter functioning in parallel with a Na/H antiporter on the basolateral membrane of the rat cortical TAL.

Methods

In this study, the technique of in vitro microperfusion of isolated rat cortical TAL was used, as previously described (14). Male, pathogen-free Sprague-Dawley rats weighing 70–100 g (Taconic Farms, Germantown, NJ) with free access to commercial rat laboratory diet and tap water were killed by decapitation. Kidneys were quickly removed and cortical TAL segments were dissected from thin (~ 1 mm) coronal slices. The tubules were dissected in the cooled (4°C) control solution of the respective experiment (Table I). The tubules were transferred into a bath chamber with a volume of ~ 150 μl. The bath fluid was continuously exchanged at 10 ml/min by hydrostatic pressure. With this setup, a complete fluid exchange can be achieved within ~ 1

Address reprint requests to Dr. Krapf, 1065 HSE, Division of Nephrology, University of California, San Francisco, CA 94143-0532.

Received for publication 2 October 1987 and in revised form 8 December 1987.

1. *Abbreviations used in this paper:* BCECF, (2',7')-*bis*-carboxyethyl)-(5,6)-carboxyfluorescein; SITS, 4-acetamido-4' isothiocyanostilbene-2,2'-disulfonate; TAL, thick ascending limb(s).

J. Clin. Invest.

0021-9738/88/07/0234/08 $2.00
Volume 82, July 1988, 234–241

s, as described previously (15, 16). Bath pH was monitored continuously by placing a commercial, flexible pH electrode into the bath (MI 21960, Microelectrodes Inc., Londonderry, NH). The bath solutions were prewarmed to 37°C and equilibrated with CO_2/O_2. Bath temperature of 37±0.5°C was maintained by a specially designed heater (glass tubing surrounded by a coiled high resistance wire) placed in-line just before the bath chamber.

To minimize motion, the distal end of the tubule was sucked gently into a collection pipette. In addition, the average tubule length exposed to the bath fluid was limited to ~ 250 μm. The tubules were allowed to equilibrate at 37°C for ~ 30 min during which they were loaded with the acetoxymethyl derivative of BCECF (BCECF-AM, Molecular Probes, Eugene, OR) from the bath in a concentration of 10 μM. Loading was continued until a signal to background fluorescence at the 450 nm excitation wavelength of ≥ 20:1 was achieved, usually requiring 10–15 min.

The perfusion solutions used in this study are listed in Table I. CO_2/HCO_3-free solutions were bubbled with 100% oxygen passed through 3 N KCN as a base trap. With these precautions bath total CO_2 is zero (15). 4-Acetamido-4′-isothiocyanostilbene-2,2′-disulfonate (SITS) was obtained from International Chemical and Nuclear (Cleveland, OH). Amiloride, nigericin, valinomycin, and all solution salts were purchased from Sigma Chemical Co. (St. Louis, MO).

Cell pH measurement. Measurements were made with an inverted fluorescent microscope (Fluovert, E. Leitz, Wetzlar, Federal Republic of Germany) using a × 25 objective as previously described (15, 16). An adjustable measuring diaphragm was appropriately placed over the tubule and opened to a rectangle of ~ 10 × 40-μm side lengths. Background fluorescence was measured before loading the tubule with the dye. After this measurement the measuring diaphragm was left in place for the entire experiment.

Analysis. BCECF has a peak excitation at 504 nm that is pH sensitive and an isosbestic point at 436 nm, where fluorescence is independent of pH. Peak emission is at 526 nm (17). Fluorescence was measured, as previously described (15–17) alternately at 500- and 450-nm excitation and at an emission wavelength of 530 nm (interference filters, Corion Corp., Holliston, MA). After correcting all measurements for background, the mean of two 500-nm excitation measurements was divided by the 450-nm excitation measurement between them, thereby yielding the fluorescence excitation ratio (F_{500}/F_{450}). For each determination, these measurements were performed twice and their mean used to estimate cell pH. The use of the ratio provides a measurement that is unaffected by changes in dye concentration (18). After a solution change, steady-state cell pH values were determined when the 500-nm excitation fluorescence had stabilized. Fluorescence was not affected by addition of amiloride (peak excitation/emission: 364/418 nm) or SITS (peak excitation/emission: 348/416 nm).

To measure the initial acidification rate (dpH_i/dt) in response to an experimental maneuver, fluorescence was followed at 500 nm while a fluid exchange was performed, and recorded on a chart recorder (LS 52, Linseis Inc., Princeton Junction, NJ). The slope of a line drawn tangent to the initial deflection (dF_{500}/dt) defined the initial rate of change in 500-nm fluorescence. By measuring fluorescence at 450 nm before and after the fluid exchange, the actual value of the 450-nm excitation at the time of the initial deflection of 500 nm could be interpolated. The rate of change in the fluorescence ratio was then calculated using the formula: $d(F_{500}/F_{450})/(dt) = (dF_{500}/dt)/(F_{450})$.

Dye calibration. In order to correlate the fluorescence excitation ratios with cell pH, the dye was calibrated intracellularly using the method of Thomas et al. (18). Tubules were perfused with well-buffered solutions (25 mM Hepes, 32 mM phosphate) containing nigericin (a K/H antiporter, 7 μM) and 64 mM potassium. Inasmuch as there are no data on the intracellular potassium activity for the rat cortical TAL, we used the values as reported for the rat distal tubule (46.5 mM, activity coefficient 0.73, Khuri et al. [19]).

Because of the uncertainties regarding the intracellular potassium activity, 5 μM valinomycin was added to the calibration solutions. In

Table I. Perfusion Solutions

	Solution																				
	1	2	3	4	5	6	7	8	9	10	11	12	13	14	15	16	17	18	19	20	21
	mmol/liter																				
Na^+	147	147		147		147	147			100	100	100	100	50	50	50	50	100	0	100	0
K^+	5	5	5	5	5	5	5	5	5	5	50	5	50	5	5	5	5	5	5	50	50
Mg^{2+}	1	1	1	1	1	1	1	1	1	1	1	1	1	1	1	1	1	1	1	1	1
Ca^{2+}	1.8	1.8	1.8	9.4	9.4	1.8	1.8	1.8	1.8	1.8	1.8	9.4	9.4	1.8	1.8	1.8	1.8	9.4	9.4	9.4	9.4
Cholin$^+$			145		25			145	145	45				95	75	95	75		25		25
N-methyl-glutamate$^+$					120							45			20		20	45	120		75
NH_4^+										±2	±2	±2	±2								
Ba^{2+}														137.8	137.8	126.6	126.6				
Cl	128.6	148.6	126.6			114.8	139.8	112.8	137.8	128.6	128.6					25	25	25	25	25	25
HCO_3^-	25	5	25	25	25	25		25		25	25	25	25								
HP_4^-	1	1	1	1	1	1	1	1	1	1	1	1	1	1	1	1	1	1	1	1	1
SO_4^-	1	1	1	1	1	1	1	1	1					1	1	1	1	1	1	1	1
Hepes$^-$						13.8	13.8	13.8	13.8					13.8	13.8						
Gluconate$^-$				143.8	141.8							143.8	143.8					141.8	141.8	141.8	141.8
Glucose	5	5	5	5	5	5	5	5	5	5	5	5	5	5	5	5	5	5	5	5	5
Hepes						11.2	11.2	11.2	11.2					11.2	11.2						

this setting, changes in potassium concentration from 64 to 128 mM at pH 7.3 did not affect the excitation ratios (n = 3). Prior to exposure to nigericin, the tubules were loaded with BCECF and then perfused with the above solutions at different pH values from the lumen and the bath or the bath only. Both methods gave similar results. Fig. 1 shows the calibration curve with the results of 13 tubules. Since these studies established a linear relationship between the fluorescence excitation ratios and pH values from 6.7 to 7.5, each tubule was calibrated individually with a two-point calibration procedure (usually at pH 7.5 and 6.7) at the end of the experiments.

Statistics. All studies were paired. After completion of the first protocol the tubules were left to equilibrate in the control solution of the second protocol for at least 5 min. The data were analyzed using the paired t test. The calibration data were fit using linear regression. Results are reported as means±standard error of the mean.

Results

Effect of peritubular pH on cell pH. In the first set of studies, the effect of changes in peritubular pH on cell pH was examined. Tubules were perfused and bathed with a control solution containing 25 mM bicarbonate (pH 7.4, solution 1, Table I). In the experimental period, the bath was changed to a solution containing 5 mM bicarbonate (pH 6.8, solution 2, Table I). In each tubule, this experiment was performed in the absence and presence of 1 mM bath SITS. Fig. 2 shows that the cells acidified by 0.31±0.02 pH units in the absence, but by only 0.18±0.02 pH units in the presence of SITS ($P < 0.005$, n = 11). In the control condition (bath pH 7.4), addition of SITS significantly alkalinized the cells from 7.10±0.06 to 7.17±0.05 ($P < 0.0025$). The acidification rate induced by lowering bath bicarbonate was also inhibited by SITS from 0.56±0.08 to 0.20±0.05 pH units/min ($P < 0.001$). These experiments demonstrate the existence of a stilbene-inhibitable basolateral pathway for movement of $H/OH/HCO_3$ ions.

Effect of peritubular sodium on cell pH. To examine the effect of peritubular sodium on cell pH, tubules were perfused and bathed with 25 mM bicarbonate and 147 mM sodium (pH 7.4, solution 1, Table I). During the experimental period, sodium was removed from the bath and replaced with choline (pH 7.4, solution 3, Table I). As before, this experiment was performed in the same tubule both in the absence and presence of 1 mM bath SITS. As shown in Fig. 3 and illustrated by the original tracing in Fig. 4 (*left sides*), bath sodium removal acidified the cells by 0.28±0.03 pH units. The initial acidification rate was 0.33±0.04 pH units/min (n = 10). The right side of Fig. 3 (compare Fig. 4 for original tracing) shows that SITS reduced the decrease in cell pH to 0.07±0.02 pH units (P < 0.001). SITS inhibited the acidification rate to 0.07±0.02 pH units/min ($P < 0.001$). Again, addition of SITS to the control solution significantly alkalinized the cells from 7.10±0.04 to 7.14±0.04 ($P < 0.025$).

To examine whether this stilbene-sensitive cell acidification induced by bath sodium removal was dependent on the presence of chloride, cell pH was measured when bath sodium was removed in the presence or absence of chloride. In the presence of chloride, cell pH decreased by 0.27±0.05 pH units when bath sodium was removed (solutions 1 and 3, Table I). In the absence of chloride, bath sodium removal (solutions 4 and 5, Table I) acidified the cells by 0.37±0.06 pH units (n = 6, NS). In chloride-free conditions, SITS had a similar effect on sodium removal–induced cell acidification as when chloride had been present: Fig. 5 illustrates that bath sodium removal (solutions 4 and 5, Table I) acidified the cells by 0.41±0.05 pH units in the absence of SITS, but by only 0.10±0.03 pH units when 1 mM SITS was present in the bath ($P < 0.001$, n = 6) and SITS also inhibited the rate of acidification from 0.30±0.06 to 0.07±0.02 pH units/min ($P < 0.0025$). These studies demonstrate that cell acidification occurs upon bath sodium removal, which is stilbene sensitive and chloride independent.

Evidence for coupling of sodium and pH effects on cell pH. The above findings could be explained if a Na/HCO_3 cotrans-

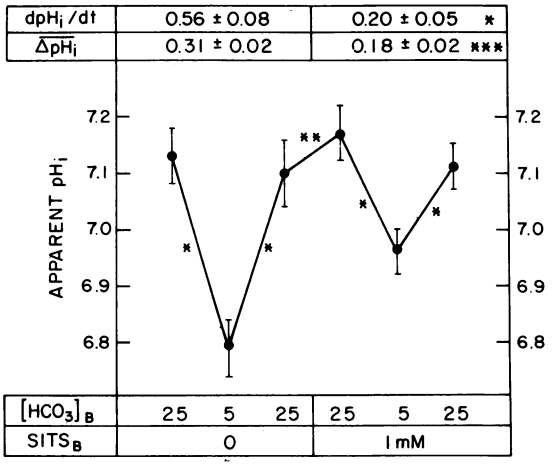

Figure 2. Effect of lowering bath HCO_3 on cell pH (pH_i) and acidification rate (dpH_i/dt). Bath HCO_3 was lowered from 25 to 5 mM (Δbath pH 7.4–6.8) in the absence and presence of 1 mM bath SITS. *$P < 0.001$; **$P < 0.0025$; ***$P < 0.005$.

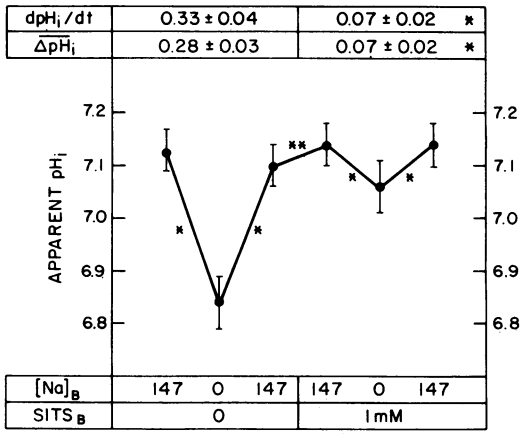

Figure 3. Effect of bath sodium removal on cell pH (pH_i) and acidification rate (dpH_i/dt). Bath sodium was replaced by choline in the absence and presence of 1 mM bath SITS. *$P < 0.001$; **$P < 0.025$.

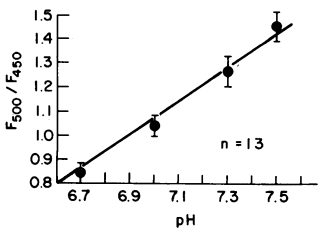

Figure 1. Intracellular dye calibration: calibration curve with the results from 13 tubules.

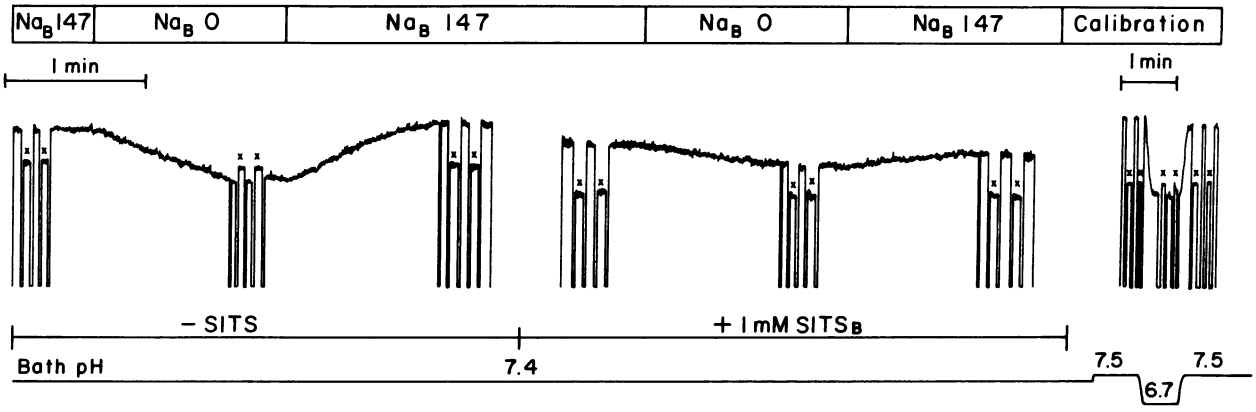

Figure 4. Effect of bath sodium removal on fluorescence excitation ratio (F_{500}/F_{450}): typical study. Changes in fluorescence are followed at 500-nm excitation wavelength. Bars marked with × denote measurements at 450-nm excitation wavelength. The study is performed in the absence (*left side*) and presence (*right side*) of 1 mM bath SITS. SITS markedly slows the change in 500-nm fluorescence and inhibits the decrease in the F_{500}/F_{450} ratio. Bath pH is monitored continuously. At the end of the experiment, the tubule is calibrated at pH 7.5 and 6.7. Note difference in time scale between experiment and calibration.

port mechanism existed on the basolateral membrane of the TAL. Such a transporter was initially described by Boron and Boulpaep (20) in the salamander proximal tubule. If this were the case, symmetric sodium removal should inhibit the effects of peritubular pH on cell pH. In addition, since this cotransporter has an absolute requirement for CO_2/HCO_3 (at least in the mammalian proximal tubule, Krapf et al. [15]), the effects of bath sodium removal on cell pH should be inhibited in the absence of CO_2/HCO_3.

When sodium was removed from luminal and bath perfusates, the cells acidified from 7.09±0.05 to 6.79±0.09 ($n = 6$, $P < 0.001$). This degree of acidification was stable and fully reversible. No late alkalinization was observed as has been reported for other nephron segments (17, 21, 22). This degree of acidification markedly decreases intracellular base concentration thereby reducing the driving force across any base exit mechanisms. Thus, the demonstration that sodium removal inhibits the effects of lowering bath HCO_3 on cell pH would have been unconvincing. Therefore, the effects of bath sodium removal were examined in the presence and absence of CO_2/HCO_3. Tubules were first perfused and bathed with 25 mM bicarbonate and 147 mM sodium and then bath sodium was removed in the experimental period (solutions 6 and 8, Table I). The experiment was then repeated with CO_2/HCO_3-free solutions (solutions 7 and 9, Table I). To minimize endogenous supply of bicarbonate, 0.1 mM acetazolamide was added to lumen and bath solutions (periods with absence of CO_2/HCO_3 only, Krapf et al. [15]). In addition, because further studies had provided evidence for a Na/H antiport mechanism on this membrane (see below), 1 mM amiloride was present in the bath throughout, both in the presence and absence of CO_2/HCO_3. The results of this study are shown in Fig. 6. Removal of CO_2/HCO_3 abolished most of the cell acidification induced by bath sodium removal. Thus, this study provides evidence for a coupling of sodium and pH effects on cell pH. In addition, this Na/base cotransport system is dependent on CO_2/HCO_3, suggesting that HCO_3 is the transported base species.

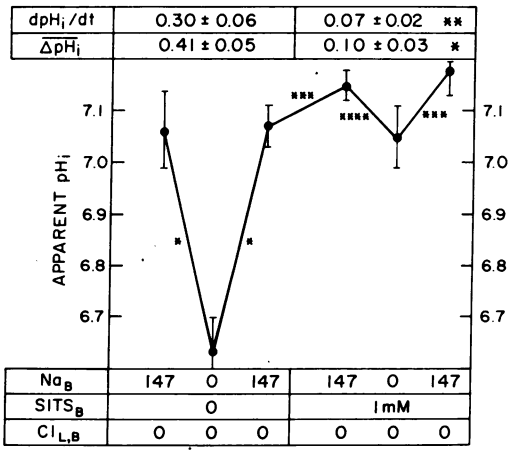

Figure 5. Effect of bath sodium removal on cell pH (pH_i) and acidification rate (dpH/dt) in the absence of chloride. The studies were performed in the absence and presence of 1 mM bath SITS. *$P < 0.001$; **$P < 0.0025$; ***$P < 0.005$; ****$P < 0.05$.

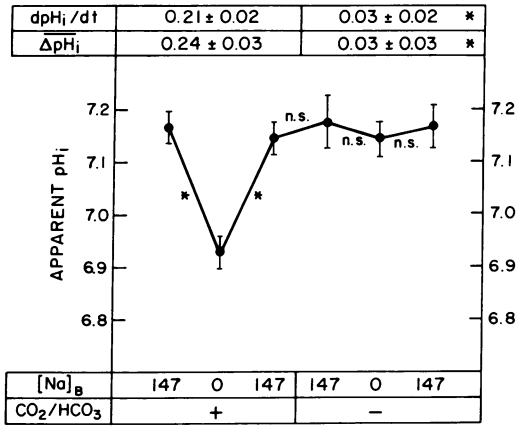

Figure 6. Effect of bath sodium removal in the presence (*left side*) and absence (*right side*) of CO_2/HCO_3 on cell pH (pH_i) and acidification rate (dpH_i/dt). 1 mM bath amiloride was present throughout the study. In the period without CO_2/HCO_3, 0.1 mM acetazolamide was added to luminal and bath fluids to minimize endogenous supply of HCO_3 from metabolism (15). *$P < 0.001$.

Evidence for electrogenicity of Na/HCO_3 cotransport. An increase in peritubular potassium causes a barium-sensitive cell membrane depolarization in the TAL (23, 24). If the TAL basolateral Na/HCO_3 cotransporter were rheogenic, as in the proximal tubule (17, 20, 25–29), depolarization of the basolateral membrane by increased peritubular potassium should alkalinize the cell. In addition, this effect should be barium sensitive. Fig. 7 shows that a step increase in bath potassium from 5 to 50 mM (solutions 10 and 11, Table I) alkalinized the cells by 0.11±0.02 pH units ($n = 6$). Addition of 2 mM bath barium also alkalinized the cells from 7.21±0.02 to 7.24±0.02 ($P < 0.02$), but blocked the effect of increasing bath potassium on cell pH ($\Delta pH_i = -0.02 \pm 0.02$, $P < 0.001$).

Barium is generally considered a specific inhibitor of a K conductance. However, studies in the rabbit cortical TAL have suggested a barium-sensitive KCl symporter on the basolateral membrane of the rabbit cortical TAL (23). It can be reasoned, therefore, that increases in bath potassium could increase cell chloride, which, in the presence of a basolateral Cl/HCO_3 exchange mechanism, could drive HCO_3 entry across this exchanger and thus alkalinize the cells. Therefore, control experiments were performed in the symmetrical absence of chloride. In four tubules, perfused with zero chloride-solutions in all periods (solutions 12 and 13, Table I), an increase in peritubular potassium alkalinized the cells by 0.20±0.02 pH units in the absence, but by only 0.05±0.03 in the presence of 2 mM bath barium ($P < 0.005$). Thus, the cell alkalinization induced by increases in bath potassium concentration is secondary to cell depolarization and is compatible with a chloride-independent, electrogenic base exit mechanism.

Effect of basolateral voltage clamp on cell acidification induced by bath sodium removal. The above results are compatible with sodium-coupled, electrogenic HCO_3 transport, but do not differentiate between an electrogenic Na/HCO_3 cotransporter or parallel Na and HCO_3 conductances. In the presence of a voltage clamp across the basolateral membrane, bath sodium removal should not acidify the cells if there were parallel conductances, whereas, a persistent acidification would be expected in the case of a Na/HCO_3 cotransporter. Tubules were therefore perfused with 100 mM sodium which was removed from the bath in the experimental period. There was zero chloride in all periods. The effect of bath sodium removal on cell pH was recorded with normal extracellular potassium (5 mM) or when the basolateral membrane voltage was clamped using 50 mM potassium and 15 μM valinomycin (the lumen always contained 5 mM potassium, solutions 18–21, Table I). As shown by Fig. 8 (*left side*), the cells acidified by 0.30±0.06 pH units without a voltage clamp and by 0.15±0.05 in the presence of a voltage clamp ($P < 0.005$, $n = 5$). Application of the voltage clamp alkalinized the cells by 0.21±0.06 pH units from 7.09±0.06 to 7.30±0.07 ($P < 0.001$).

In five additional tubules, the experiments were repeated in the presence of 1 mM bath amiloride to inhibit a basolateral Na/H antiporter (see below) and a possible sodium conductance. As illustrated by Fig. 8 (*right side*), there was a significant persistent acidification after voltage clamp. The cells acidified by 0.25±0.07 pH units when bath sodium was removed in the absence of a voltage clamp and by 0.12±0.02 in its presence ($P < 0.005$). Again, application of the voltage clamp alkalinized the cells by 0.25±0.05 pH units from 7.10±0.06 to 7.35±0.11 ($P < 0.001$). Thus, these results suggest a Na/HCO_3 cotransporter and argue against parallel conductances. The smaller acidification after voltage clamp may be due to the fact that this experiment eliminated the electrical driving force across this transporter and possibly lowered cell sodium activity secondary to cell alkalinization. A cell alkalinization of this magnitude can be expected to inhibit the rates of the luminal and basolateral Na/H antiporters (see below). When potassium and valinomycin where increased to 64 mM and 20 μM, respectively, the persistent acidification was of a similar degree, suggesting that the voltage clamp by 50 mM potassium/15 μM valinomycin was adequate (two tubules).

Effect of amiloride on sodium-dependent $H/OH/HCO_3$ transport. The fact that SITS inhibition of the effects of bath sodium and HCO_3 changes on cell pH was incomplete (Figs. 2 and 3) suggested the presence of a SITS-insensitive, sodium-dependent process on the basolateral membrane of the cortical TAL. The next experiments were therefore designed to test for the presence of an amiloride-sensitive Na/H antiporter. In the first group of studies, the effect of 1 mM bath amiloride on the cell pH recovery from an acid load was examined. In the absence of exogenous CO_2/HCO_3, tubules were exposed to a bath solution containing 20 mM of NH_3/NH_4. A bath fluid exchange back to a NH_3/NH_4 free solution was then performed (solutions 14 and 15, Table I). Due to its high permeability, NH_3 diffuses rapidly out of the cells leaving behind protons, which represent the acid load to the cells (30). The

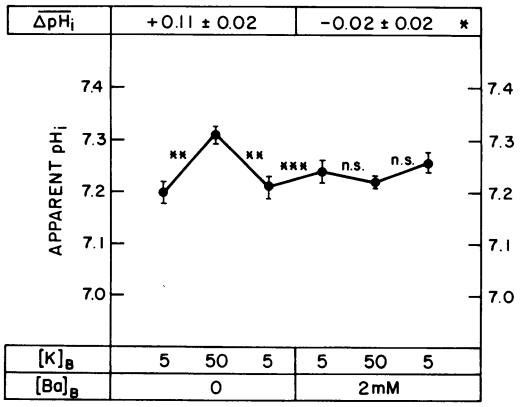

Figure 7. Effect of increasing bath potassium concentration from 5 to 50 mM on cell pH (pH_i). The study was performed in the presence and absence of 2 mM bath barium. $^*P < 0.001$; $^{**}P < 0.025$; $^{***}P < 0.02$.

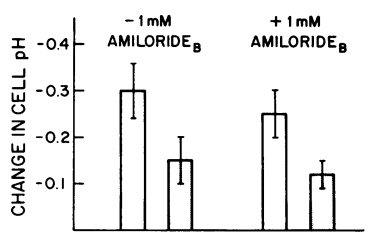

Figure 8. Cell pH changes induced by bath sodium removal from 100 to 0 mM in the absence (*open bars*) and presence (*hatched bars*) of a basolateral voltage clamp (50 mM potassium, 15 μM valinomycin). The study was performed in the bilateral absence of chloride. The two bars on the left represent results from five tubules in the absence of bath amiloride, the two bars on the right are results from five tubules where 1 mM bath amiloride was present. There is a significant persistent acidification under voltage-clamped conditions that is amiloride insensitive.

rate of cell pH recovery was then analyzed in the presence and absence of 1 mM bath amiloride. Because amiloride competes with sodium for the sodium-binding sites on the transporter, tubules were perfused in lumen and bath with solutions containing 50 mM sodium (31). As shown in Fig. 9 (*left side*), amiloride significantly inhibited the cell pH recovery from this acid load. The rate of cell pH recovery was reduced from 0.16±0.03 to 0.02±0.06 pH units/min ($n = 6$, $P < 0.002$). The steady-state cell pH value before addition and removal of NH_3/NH_4 was 7.02±0.03 in the absence and 7.03±0.02 in the presence of amiloride. Similar experiments were also performed in the presence of exogenous CO_2/HCO_3 (solutions 16 and 17, Table I). In this setting, the cells recovered from the acid load with a rate of 0.06±0.02 pH units/min. As illustrated on Fig. 9 (*right side*), 1 mM bath amiloride inhibited the recovery rate to 0.02±0.01 pH units/min ($n = 5$, $P < 0.01$). Again, amiloride did not affect steady-state cell pH values significantly (7.15±0.07 in the absence vs. 7.21±0.06 in the presence of amiloride).

Thus, these studies provide evidence for a basolateral amiloride-sensitive Na/H antiporter involved in cell pH response to an acid load. The slower recovery rate in the presence of exogenous CO_2/HCO_3 is probably due to the fact that the rapid NH_3 washout acidifies the cells to a lesser degree in the presence of exogenous CO_2/HCO_3 due to the higher cellular buffering power. The ammonia washout acidified the cells to 6.64±0.10 in the absence of CO_2/HCO_3 and to 6.86±0.09 in the presence of CO_2/HCO_3. Thus, it is conceivable that the Na/H antiporter was less stimulated in the presence of CO_2/HCO_3.

To investigate the possibility whether cell acidification induced by bath sodium removal is also amiloride sensitive, tubules were perfused symmetrically with solutions containing 50 mM sodium. Sodium was then removed from the bath in the absence and presence of 1 mM bath amiloride (solutions 3 and 16, Table I). Fig. 10 shows that amiloride had a small, but statistically significant inhibitory effect on cell acidification induced by bath sodium removal. The cells acidified by 0.12±0.03 pH units in the absence, but by only 0.07±0.02 in the presence of amiloride ($n = 6$, $P < 0.005$). Amiloride slowed the cell acidification rate from 0.14±0.03 to 0.08±0.03 pH units/min ($P < 0.01$).

Thus, it can be concluded that this amiloride-sensitive Na/H antiporter is also sensitive to changes in bath sodium concentration.

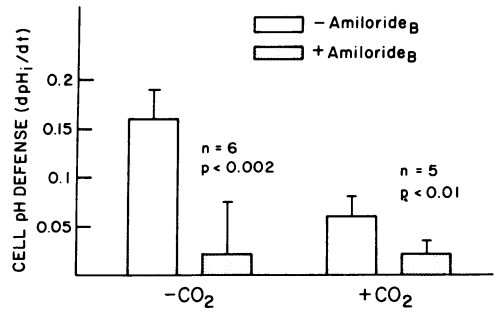

Figure 9. Rates of cell pH defense against an acid load (rapid ammonia washout) in the absence (two bars on the left) and presence (two bars on the right) of CO_2/HCO_3: effect of 1 mM bath amiloride.

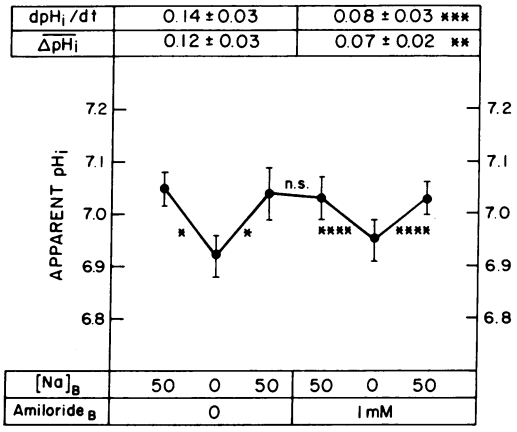

Figure 10. Effect of bath sodium removal (50 to 0 mM) on cell pH (pH_i) and acidification rate (dpH_i/dt). The experiments were performed in the absence and presence of 1 mM bath amiloride. *$P <$ 0.0025; **$P < 0.005$; ***$P < 0.01$, ****$P < 0.04$.

Discussion

In this study, the technique of microfluorometric determination of cell pH (15, 17) using the fluorophore BCECF was adapted to the in vitro microperfused, rat cortical TAL. The following were the key observations: (*a*) lowering peritubular HCO_3 or sodium induced a stilbene-sensitive cell acidification (Figs. 2, 3, and 4); (*b*) stilbene addition alkalinized the cells (Figs. 2, 3, and 5); (*c*) cell acidification induced by peritubular sodium removal was independent of chloride but was inhibited in the absence of CO_2/HCO_3 (Figs. 5 and 6); (*d*) cell depolarization (induced by raising peritubular potassium concentration) lead to a barium-sensitive, chloride-independent cell alkalinization (Fig. 7); and (*e*) cell acidification induced by bath sodium removal persisted when the basolateral membrane voltage was clamped with high potassium/valinomycin (Fig. 8). All of these findings are consistent with the presence of an electrogenic $Na/(HCO_3)_{n>1}$ cotransport mechanism on the basolateral membrane of the rat cortical TAL.

In previous studies in the rat proximal convoluted tubule (17, 22) and rabbit proximal S3 segment (21), bilateral sodium removal initially acidified the cells (consistent with stopping luminal Na/H exchange), which was followed by late cell alkalinization. This late alkalinization was probably due to some sodium-independent proton extrusion, possibly via an H-ATPase. In the present study, bilateral sodium removal acidified the cells by 0.3 pH units without evidence for a late alkalinization. This suggests that the rates of sodium-dependent transporters on both sides of the cortical TAL cells are the major determinants of cell pH.

Because of the associated cell acidification it was not possible to address the question whether the cell alkalinization induced by increases in bath potassium is inhibited by sodium removal. In addition to associated decreases in cellular base concentration, such cell pH changes are known to markedly affect the cell membrane potential (32, 33). These complicating factors render such an experiment impossible to interprete without exact knowledge of the membrane potential difference changes. However, the following results from these studies suggest the presence of an electrogenic Na/HCO_3 cotrans-

porter rather than parallel sodium and HCO_3 conductances: (*a*) There was a significant, amiloride-insensitive cell acidification when bath sodium was removed in the presence of a clamped basolateral membrane voltage (Fig. 8) and (*b*) 1 mM bath amiloride failed to affect cell pH significantly. This concentration of amiloride is above those shown to inhibit known epithelial sodium channels (34). If there were a basolateral sodium conductance in parallel with a HCO_3 conductance, the inward gradient for sodium would tend to depolarize the cell membrane; amiloride should hyperpolarize the cell membrane, increase the driving force for base exit, and acidify the cell. There was no effect of amiloride on cell pH both at sodium concentrations of 50 and 147 mM in these studies.[2]

The facts that cell pH defense against an acid load was inhibited by bath amiloride both in the presence and absence of CO_2/HCO_3 (Fig. 9) and that amiloride also exerted an inhibitory effect on cell acidification induced by bath sodium removal (Fig. 10) provide evidence for a Na/H antiporter in parallel with the $Na/(HCO_3)_{n>1}$ cotransporter. This combination of transporters has been described previously on the basolateral membrane of the amphibian proximal tubule (20, 35). Hebert (11) has also found evidence for a Na/H antiporter on the basolateral membrane of the mouse medullary TAL. This transporter, in parallel with a Cl/HCO_3 exchanger, seems important in vasopressin-dependent hypertonic volume regulation in this segment. Although the intracellular sodium activity in the rat cortical TAL is unknown,[3] it is reasonable to assume that it is ~ 10–20% of the extracellular activity. Given a cell pH of 7.13, as determined in these studies, the driving forces dictate proton extrusion into the basolateral compartment by the Na/H antiporter and would thus oppose the net effect of the $Na/(HCO_3)_{n>1}$ cotransporter. In addition, this basolateral Na/H antiporter would also be counterproductive to the net sodium reabsorption in this segment. It is clear, however, that for net sodium-dependent HCO_3 reabsorption to occur (3, 4), sodium-coupled base exit has to dominate the Na/H antiporter activity. It is important to realize that bath sodium removal induced only very small changes in cell pH and acidification rate after SITS inhibition (in the presence and absence of chloride; see Figs. 3 and 5). Thus, even if one assumes 100% inhibition by SITS, the rate of the Na/H antiporter is very slow (acidification rate after SITS inhibition below 0.07 pH units/min). Therefore, the role of this transporter in transcellular H/OH transport is probably small. However, an important role in cell pH defense is suggested by the interesting finding that bath amiloride markedly inhibited cell pH defense against an acid load (Fig. 9). The luminal Na/H antiporter (3) would also be expected to contribute importantly to cell pH defense in this setting and the marked degree of inhibition of cell pH defense by bath amiloride alone is surprising. Preliminary evidence from our laboratory directly confirms the presence of a luminal Na/H antiporter in the rat cortical TAL.[4] Therefore, the relative importance of luminal and basolateral Na/H antiporters in determination of cell pH and cell pH defense need further investigation.

The failure to observe a late alkalinization after bilateral sodium removal is an argument against an important role for an H-ATPase (37) in luminal proton secretion. Such an ATPase would be expected to be stimulated by cell acidification and, since it is electrogenic, by the decrease in transepithelial voltage associated with sodium removal (3). Thus, the functional significance of a luminal H-ATPase for transcellular proton secretion and/or cell pH defense seems small but more direct studies will be needed to address this issue.

These studies do not address the possibility of sodium-dependent, chloride-coupled base transport mechanisms (22, 38, 39). Since there is now evidence for an electrogenic Na/HCO_3 cotransporter and the basolateral membrane is conductive for chloride in the mammalian TAL (40), analysis of chloride-coupled base transport mechanisms will require specific information about changes in the basolateral membrane potential.

In conclusion, these studies provide evidence for the existence of an electrogenic $Na/(HCO_3)_{n>1}$ cotransporter in parallel with a Na/H antiporter on the basolateral membrane of the rat cortical TAL. The results suggest a major role in basolateral HCO_3 transport for the $Na/(HCO_3)_{n>1}$ cotransporter, whereas the Na/H antiporter may be more important in cell pH defense.

Acknowledgments

The author is grateful to Drs. F. C. Rector, Jr., and C. A. Berry for support and advice.

The author is the recipient of a generous grant from the Swiss Foundation for medical and biological grants. This study was supported by grants DK-27945 and DK-26142 from the National Institutes of Health.

References

1. DuBose, T. D., L. R. Pucacco, M. S. Lucci, and N. W. Carter. 1979. Micropuncture determination of pH, P_{CO_2} and total CO_2 concentration in accessible structures of the rat renal cortex. *J. Clin. Invest.* 64:476–482.

2. Buerkert, J., D. Martin, and D. Trigg. 1983. Segmental analysis of the renal tubule in buffer production and net acid formation. *Am. J. Physiol.* 244(Renal Fluid Electrolyte Physiol. 13):F442–F454.

3. Good, D. W. 1985. Sodium-dependent bicarbonate absorption by cortical thick ascending limb of rat kidney. *Am. J. Physiol.* 248(Renal Fluid Electrolyte Physiol. 17):F821–F829.

4. Good, D. W., M. A. Knepper, and M. B. Burg. 1984. Ammonia and bicarbonate transport by thick ascending limb of rat kidney. *Am. J. Physiol.* 247(Renal Fluid Electrolyte Physiol. 16):F35–F44.

5. Iino, Y., and M. B. Burg. 1981. Effect of acid-base status in vivo on bicarbonate transport by rabbit renal tubules in vitro. *Jpn. J. Physiol.* 31:99–107.

6. Dobyan, D. C., L. S. Magill, P. A. Friedman, S. C. Hebert, and R. E. Bulger. 1982. Carbonic anhydrase histochemistry in rabbit and mouse kidneys. *Anat. Rec.* 204:185–197.

2. Addition of 1 mM bath amiloride to four tubules perfused with 147 mM (solution 1, Table I) had no effect on cell pH: 7.11±0.03 in the absence as compared to 7.12±0.04 (NS) in the presence of amiloride.

3. Intracellular sodium activity has been measured only in the amphibian diluting segment and was found to be between 10 and 12 mmol/liter (36).

4. When lumen and bath were perfused with 147 mM sodium at pH 7.4 and luminal sodium was removed in the experimental period (solutions 1 and 3, Table I), the cells acidified by 0.14±0.02 pH units in the absence and by 0.04±0.02 pH units in the presence of 1 mM luminal amiloride (n = 5 tubules).

7. Loennerholm, G., and Y. Ridderstrale. 1980. Intracellular distribution of carbonic anhydrase in the rat kidney. *Kidney Int.* 17:162–174.

8. Loennerholm, G., and P. J. Wistrand. 1984. Carbonic anhydrase in the human kidney: a histochemical and immunocytochemical study. *Kidney Int.* 25:886–898.

9. Friedman, P. A., and T. E. Andreoli. 1982. CO_2-stimulated NaCl absorption in the mouse renal cortical thick ascending limb of Henle. *J. Gen. Physiol.* 80:683–711.

10. Oberleithner, H. 1985. Intracellular pH in diluting segment of frog kidney. *Pfluegers Arch. Eur. J. Physiol.* 404:244–251.

11. Hebert, S. C. 1986. Hypertonic cell volume regulation in mouse thick ascending limbs. II. Na/H and Cl/HCO_3 exchange in basolateral membranes. *Am. J. Physiol.* 250(Cell. Physiol. 19):C920–C931.

12. Wang, W., P. Dietl, and H. Oberleithner. 1987. Evidence for a Na-dependent rheogenic HCO_3 transport in fused cells of frog distal tubules. *Pfluegers Arch. Eur. J. Physiol.* 408:291–299.

13. Wang, W., P. Dietl, S. Silbernagl, and H. Oberleithner. 1987. Cell membrane potential: a signal to control intracellular pH and transepithelial hydrogen ion secretion in frog kidney. *Pfluegers Arch. Eur. J. Physiol.* 409:289–295.

14. Burg, M. B., J. Grantham, M. Abramow, and J. Orloff. 1966. Preparation and study of fragments of the single rabbit nephron. *Am. J. Physiol.* 210:1293–1298.

15. Krapf, R., R. J. Alpern, F. C. Rector, Jr., and C. A. Berry. 1987. Basolateral membrane Na/base cotransport is dependent on CO_2/HCO_3 in the proximal tubule. *J. Gen. Physiol.* 90:833–853.

16. Krapf, R., R. J. Alpern, C. A. Berry, and F. C. Rector, Jr. 1988. Regulation of cell pH by ambient HCO_3, P_{CO_2} and pH in the rabbit proximal convoluted tubule. *J. Clin. Invest.* 81:381–389.

17. Alpern, R. J. 1985. Mechanism of basolateral membrane H/OH/HCO_3 transport in the rat proximal convoluted tubule. *J. Gen. Physiol.* 86:613–636.

18. Thomas, J. A., R. N. Buchsbaum, A. Zimnik, and F. Racke. 1979. Intracellular pH measurements in Ehrlich ascites tumor cells utilizing spectroscopic probes generated in situ. *Biochemistry.* 18:2210–2218.

19. Khuri, R. N., S. K. Agulian, and A. Kalloghlian. 1972. Intracellular potassium in cells of the distal tubule. *Pfluegers Arch. Eur. J. Physiol.* 335:297–308.

20. Boron, W. F., and E. L. Boulpaep. 1983. Intracellular pH regulation in the renal proximal tubule of the salamander. Basolateral HCO_3 transport. *J. Gen. Physiol.* 81:53–94.

21. Nakhoul, N. L., and W. F. Boron. 1985. Intracellular pH regulation in rabbit proximal straight tubules: dependence on external sodium. *Fed. Proc.* 44:1898. (abstr.)

22. Alpern, R. J., and M. Chambers. 1987. Basolateral membrane Cl/HCO_3 exchange in the rat proximal convoluted tubule: Na-dependent and independent modes. *J. Gen. Physiol.* 89:581–598.

23. Greger, R., and E. Schlatter. 1983. Properties of the basolateral membrane of the cortical thick ascending limb of Henle's loop of rabbit kidney. *Pfluegers Arch. Eur. J. Physiol.* 396:325–334.

24. Yoshitomi, K., C. Koseki, J. Taniguchi, and M. Imai. 1987. Functional heterogeneity in the hamster medullary thick ascending limb of Henle's loop. *Pfluegers Arch. Eur. J. Physiol.* 408:600–608.

25. Yoshitomi, K., B.-Ch. Burckhardt, and E. Froemter. 1985. Rheogenic sodium-bicarbonate cotransport in the peritubular cell membrane of the rat renal proximal tubule. *Pfluegers Arch. Eur. J. Physiol.* 405:360–366.

26. Biagi, B. A., and M. Sothell. 1986. Electrophysiology of basolateral bicarbonate transport in the rabbit proximal tubule. *Am. J. Physiol.* 250(Renal Fluid Electrolyte Physiol. 19):F267–F272.

27. Grassl, S. M., and P. S. Aronson. 1986. Na/HCO_3 cotransport in basolateral membrane vesicles isolated from the rabbit renal cortex. *J. Biol. Chem.* 261:8778–8783.

28. Sasaki, S., T. Shiiga, N. Yoshiyama, and J. Takeuchi. 1987. Mechanism of bicarbonate exit across basolateral membrane of the rabbit proximal straight tubule: a microelectrode study. *Am. J. Physiol.* 252(Renal Fluid Electrolyte Physiol. 21):F11–F18.

29. Soleimani, M., S. M. Grassl, and P. S. Aronson. 1987. Stoichiometry of Na/HCO_3 cotransport in basolateral membrane vesicles isolated from the rabbit renal cortex. *J. Clin. Invest.* 79:1276–1280.

30. Roos, A., and W. F. Boron. 1981. Intracellular pH. *Physiol. Rev.* 61:296–434.

31. Kinsella, J. L., and P. S. Aronson. 1981. Amiloride inhibition of the Na/H exchanger in renal microvillus membrane vesicles. *Am. J. Physiol.* 241(Renal Fluid Electrolyte Physiol. 10):F374–F379.

32. Eaton, D. C., K. L. Hamilton, and K. E. Johnson. 1984. Intracellular acidosis blocks the basolateral Na/K pump in rabbit urinary bladder. *Am. J. Physiol.* 247(Renal Fluid Electrolyte Physiol. 16):F946–F954.

33. Biagi, B. A., and M. Sohtell. 1986. pH sensitivity of the basolateral membrane of the rabbit proximal tubule. *Am. J. Physiol.* 250(Renal Fluid Electrolyte Physiol. 19):F261–266.

34. Benos, D. J. 1982. Amiloride: a molecular probe of sodium transport in tissues and cells. *Am. J. Physiol.* 242(Cell Physiol. 11):C131–C145.

35. Boron, W. F., and E. L. Boulpaep. 1983. Intracellular regulation in the renal proximal tubule of the salamander. Na/H exchange. *J. Gen. Physiol.* 81:29–52.

36. Oberleithner, H., G. Giebisch, F. Lang, and W. Wang. 1982. Cellular mechanisms of the furosemide-sensitive transport system in the kidney. *Klin. Wochenschr.* 60:1173–1179.

37. Gluck, S., S. Hirsch, and D. Brown. 1987. Immunocytochemical localization of H-ATPase in rat kidney. *Kidney Int.* 31:167. (Abstr.)

38. Guggino, W. B., R. London, E. L. Boulpaep, and G. Giebisch. 1983. Chloride transport across basolateral cell membrane of the Necturus proximal tubule: dependence on bicarbonate and sodium. *J. Membr. Biol.* 71:227–240.

39. Grassl, S. M., P. D. Holohan, and C. R. Ross. 1987. HCO_3 transport in basolateral membrane vesicles isolated from the rat renal cortex. *J. Biol. Chem.* 262:2682–2687.

40. Greger, R. 1985. Ion transport mechanisms in thick ascending limb of Henle's loop of mammalian nephron. *Physiol. Rev.* 65:760–797.